DTU Library

Grey box modeling of supermarket refrigeration cabinets

Leerbeck, K.; Bacher, P.; Heerup, C.; Madsen, H.

Published in:
Energy and AI

Link to article, DOI:
10.1016/j.egyai.2022.100211

Publication date:
2023

Document Version
Publisher's PDF, also known as Version of record

Citation (APA):
Leerbeck, K., Bacher, P., Heerup, C., & Madsen, H. (2023). Grey box modeling of supermarket refrigeration cabinets. *Energy and AI*, *11*, Article 100211. https://doi.org/10.1016/j.egyai.2022.100211

Energy and AI 11 (2023) 100211

Contents lists available at ScienceDirect

Energy and AI

journal homepage: www.elsevier.com/locate/egyai

Grey box modeling of supermarket refrigeration cabinets ☆

K. Leerbeck [a,*], P. Bacher [a], C. Heerup [b], H. Madsen [a]

[a] DTU Compute, Bygning 324, 2800 Kongens Lyngby, Denmark
[b] Gregersensvej 2, 2630 Taastrup, Denmark

HIGHLIGHTS

- Grey box modeling of supermarket CO_2 refrigeration evaporators and cabinets.
- Analysis of physically interpretable parameter estimates.
- Classification of refrigeration cabinets based on parameter estimates characteristics.

GRAPHICAL ABSTRACT

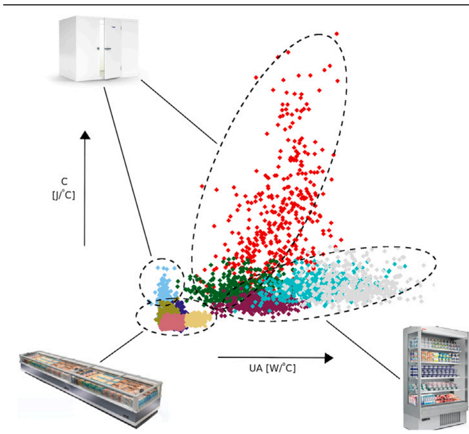

ARTICLE INFO

Keywords:
Grey box modeling
CO_2 refrigeration systems
Refrigeration cabinets and evaporators
System identification
Classification

ABSTRACT

Aiming to enable robust large-scale fault diagnostics and optimized control for supermarket refrigeration systems, a data-driven grey box model for an evaporator and its surrounding cooling cabinet (or room) is presented. It is a non-linear model with two states: the cabinet temperature and the refrigerant mass in the evaporator. To demonstrate its applicability, data with one-minute sampling resolution from ten evaporators in a supermarket in Otterup (Denmark) was used. The model parameters were estimated using a Kalman filter and the maximum likelihood method. Since the dynamical properties of the cabinets constantly change as goods are added and removed, the parameters were re-estimated for each night, over a period of approximately 2.5 years. The model is validated through a statistical analysis of the residuals and the importance of the ongoing re-estimation of parameters is highlighted. Furthermore, the physical meaning of the estimated parameters is discussed and potential applications for characterization and classification of cabinets are demonstrated, by showing how they can be differentiated as either open- or closed cabinets or rooms, using only the estimated heat transfer coefficients and heat capacities. For a selected case it is shown that the estimated parameter values are close to physics derived values, and that the accuracy measured by the standard errors of the estimates is approximately $\pm 10\%$ relative to the estimated values. The analysis demonstrates that the model is robust, accurate and reliable in terms of estimating physically meaningful parameters and it is therefore appropriate for large-scale implementation.

☆ This document is the results of the research project Digital Twins (https://digitaltwins4hprs.dk/) partly funded by the EUDP programme.

* Corresponding author.
E-mail addresses: kenle@dtu.dk (K. Leerbeck), pbac@dtu.dk (P. Bacher), chp@teknologisk.dk (C. Heerup), hmad@dtu.dk (H. Madsen).

https://doi.org/10.1016/j.egyai.2022.100211
Received 6 August 2022; Received in revised form 12 October 2022; Accepted 13 October 2022
Available online 20 October 2022

Nomenclature

Parameters

$\dot{m}$	Mass flow (kg/s)
λ	Conductivity (W/(m K))
P	Pressure (Bar)
ρ	Density (kg/m^3)
A	Valve Constant ($\sqrt{10}$ m^2)
C	Heat capacity (kWh/K)
H	Height (m)
h	Enthalpy (J/kg)
L	Thickness (m)
M	Mass (kg)
R	Thermal resistance (K/kW)
T	Temperature (°C)
W	Width (m)
UA	Heat transfer coefficient (kW/K)

Super- and subscripts

a	Ambient air
c	Air inside the cabinet (or room)
e	Evaporator
load	Surface of wall and door between the room and ambient air
m	Surface of evaporator
r	Refrigerant inside the evaporator
rec	Receiver tank

1. Introduction

To better exploit the benefits of system modeling and automation, the need for digital twins (digital representations of a physical systems) is growing, as reported for industrial systems in general by [1] and for refrigeration systems in particular by [2]. With the increasing amount and resolution of data being gathered from all sorts of sources, the potential and applications expand, opening up for new research questions to be answered. The present paper focuses specifically on data-driven modeling of supermarket refrigeration rooms and display cabinets. The presented methodology is an outcome of the continued research from the results presented in [3], where some limitations were found with the applied model and numerical implementation, e.g. lack of robustness and convergence in the estimation.

Grey box modeling – characterized by being a combination physics and statistics – of supermarket refrigeration systems is a research area of great interest and potential. The models can be used for applications in optimized control [4,5] and fault detection [6]. Thus, we achieve physical insight of the parameters of the overall and complex system using measured time series data, as described in more detail by [7,8]. Early methodologies on parameter estimation in stochastic differential equations describing a physical system have been around for many years [9], but are only recently being implemented on a large-scale with the new data era. The method has been well tested in many applications, for estimating building thermal dynamics, see [10,11], and for refrigeration system applications, see [2].

A promising approach to data-driven modeling and optimization of one-stage refrigeration systems is with neural networks and predictive control as presented in [12] to increase the efficiency of the compressor in a refrigeration system. This is later followed-up in [13], where an energy reduction of 17% was achieved on the one-stage system. However, supermarkets' refrigeration systems are usually two-stage systems with two temperature levels, one for frozen goods and one for refrigerated goods, each with its own compressor equipment, which significantly complicates the models needed.

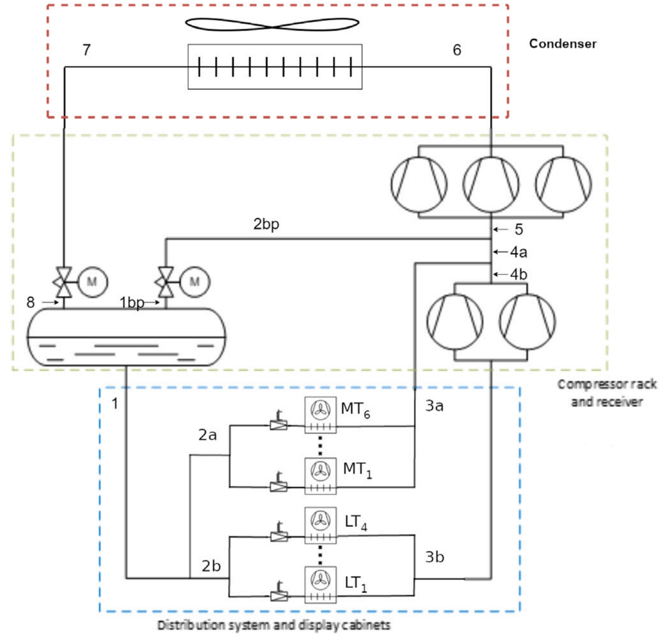

Fig. 1. Flow sheet of a supermarket CO_2 refrigeration system. The three main parts are marked on the figure. The modeled evaporators and cabinets are in the "Distribution system and display cabinets" part. On the figure measurement points are marked with numbered labels — descriptions of them are found in the main text.

Data-driven modeling of supermarket refrigeration systems can be done by modeling each single component; compressors, condensers and evaporators separately, see [14] for modeling of a compressor, [15] for evaporators and condensers, and [16] for a gas-cooler example. Alternatively, the system may be modeled as a near-complete refrigeration system with several components integrated, see [17] for modeling a vapor compression plant, [18] for phase change materials and [19] for a high heat flux removal system example. Detailed data-driven models of a complete system were developed by [20], using subspace modeling – a method for parameterization in non-linear Multiple Inlet Multiple Outlet (MIMO) systems [21]. In the particular study the refrigeration cabinets were not considered individually. Using single-component models, the parameterization can be done in higher detail, whilst having fewer parameters per model compared to single multi-component model — this makes parameter estimation easier and more reliable. Thus, a clever way to use both principles is to first parameterize separate models of the main components (e.g. refrigeration cabinets, compressors and the condenser) – this was done in [22], using Predictive Error Minimization for estimation. Afterwards, the complete system was modeled using the estimated parameters. The model was applied to develop control strategies utilizing the high heat capacity of the goods to enable demand flexibility of supermarket refrigeration systems.

A problem with previously suggested models is their lack of practical identifiability due to high model complexity. This is pointed out in [3], where an evaporator in a refrigeration room was modeled. It was shown that model over-parameterization led to physically unrealistic parameter estimates. The model predicts very well the cabinet temperature, hence it is applicable for control, however, with physically infeasible parameter estimation the system properties and energy demand cannot be determined.

The objective with the present paper is to demonstrate the benefits and potential applications from simplifying the previously applied models. The key novelty of the presented results is the application of

Fig. 2. Open display cabinet, ref.: Arneg/WICA.

Fig. 3. Closed display cabinet, ref.: Arneg/WICA.

Fig. 4. Refrigeration room, ref.: Arneg/Incold.

Table 1
Evaborators with their cabinets and valves installed in the system. The last column lists the valve constants A – derived from a previous study [23].

Cabinet	Type	Valve	$A[\sqrt{10m^2}]$
MT_1	Room	AKV 10–3	0.58765
MT_2	Room	AKV 10–5	1.48523
MT_3	Open cabinet	AKV 10–4	0.94185
MT_4	Open cabinet	AKV 10–5	1.48523
MT_5	Open cabinet	AKV 10–5	1.48523
MT_6	Closed cabinet	AKV 10–2	0.37191
LT_1	Room	AKV 10–3	0.58765
LT_2	Closed cabinet	AKV 10–2	0.37191
LT_3	Closed cabinet	AKV 10–2	0.37191
LT_4	Closed cabinet	AKV 10–2	0.37191

the simpler model with fewer parameters and the demonstration of how that ensures identifiability, and thus consistently physical meaningful parameters. The estimation results using the simpler model for each night for ten individual cabinets the parameters were re-estimated each night, in total 4143 independent estimations of the model are included in the presented results. It is shown how the estimates can be used for various applications e.g. characterization and fault detection, which would not be possible with previous presented models.

In Section 2, the supermarket refrigeration system which were modeled is presented and explained. In Section 3, the applied grey box model and method for parameter estimation are presented. In Section 4, the resulting model is illustrated using a five-hour prediction on both in-sample and out-of-sample data. Furthermore, a residual analysis is presented for validating the model. In Section 5, a potential application of the model is presented and discussed. It is shown how the model can be used for classification of the cabinet type — i.e. whether it is an open- or closed cabinet, or a room. Finally, in Section 6 the results are discussed and in Section 7 the conclusions are drawn.

2. The refrigeration system and data

The modeled cabinets are part of the supermarket refrigeration system in the store named "Fakta" in the city of Otterup, Denmark. We consider ten cabinets — six for fresh foods and four for frozen foods. The study is based on data from 2012 to 2014 where the opening hours were 8:00–21:00 every day. The system is a CO_2 booster system with a nominal cooling capacity of around 38 kW and refrigerant mass flow of 0.293 kg/s CO_2. A flow sheet of the system is presented in Fig. 1, where numbering labels mark measurement points. After the receiver, at the point marked by "1", the refrigerant is liquefied- and from there, it is split into the medium temperature evaporator (MT) string and the low temperature evaporator (LT) string, where expansion valves drop the pressure to the desired saturation temperature letting refrigerant into their corresponding evaporator. The valves are controlled with either a hysteresis or a modulating method with feedback from the measured cabinet temperature. After the evaporators, at stages "2a" and "2b", the refrigerant is superheated to avoid any droplets from entering the compressor. At stage "4a", "4b" and "5", after the low-temperature compressor rack, the pressure is the same, but the enthalpy varies as the MT string and bypass (bp) string from the receiver connects. The refrigerant now enters the high-pressure compressor rack and continues the condenser to a sub-cooled state at stage "8"- and the cycle repeats.

The present research focus on modeling each cabinet and their corresponding evaporator, hence anything between stage "6" and "8" will not be discussed further. The cabinets included in this study are listed in Table 1 with specifications. MT refers to medium temperature (fresh food) and LT refers to low temperature (frost). We distinguish between three types of cabinets: room, open- and closed cabinet (illustrated in Figs. 2–4).

The cooling energy released in each cabinet is mostly determined by the refrigerant mass flow through its corresponding evaporator. This flow is determined by the opening degree and the valve constant — the latter is a measure of the specific evaporator valve size. The valve constants must be known in advance for the parameter estimation suggested in this paper otherwise the applied model will be over-parameterized. The valve constants can also be estimated separately, as shown in [24].

2.1. Data

The study uses one-minute sampling data consisting of pressures, temperatures and valve openings measured at the numbered points on

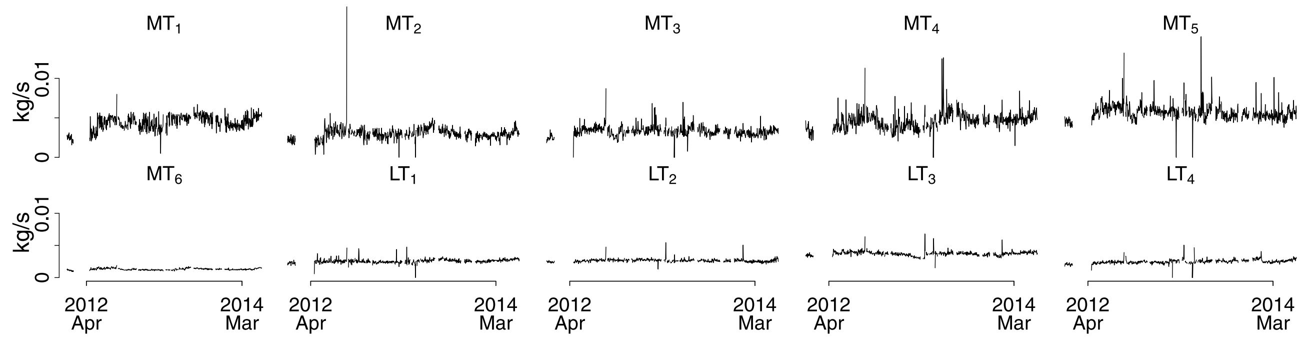

Fig. 5. Nightly averages of the mass flows entering the evaporators for each of the eight cabinets (from 00:00 AM to 4:59 AM every night in the period).

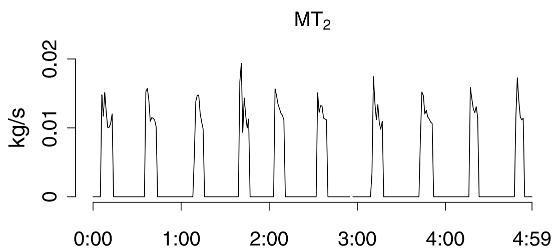

Fig. 6. The mass flow entering the evaporator of the cooling room MT_2 during 29th of October 2013. This is an example of hysteresis control, where the valve is either fully open or closed.

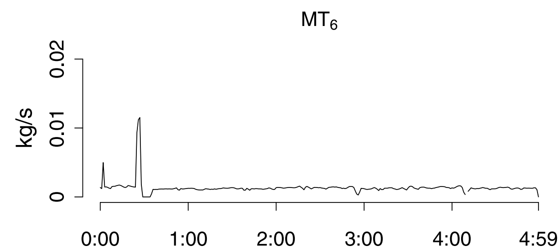

Fig. 7. The mass flow entering the evaporator of the closed cabinet MT_6 the 29th of October 2013. This is an example of modulating control, where the opening of the valve is set as a continuous value by the controller.

Fig. 1. The mass flow entering evaporator i is calculated by

$$\dot{m}_{\mathrm{in},i} = \sqrt{(P_{\mathrm{rec}} - P_{0,i})\rho_i} \cdot o_{\mathrm{d,i}} \cdot A_i \tag{1}$$

where P_{rec} is the pressure in the receiver, ρ is the refrigerant density, and for the i'th evaporator $P_{0,i}$ is the suction pressure measured at point "3a" and "3b", $o_{\mathrm{d,i}}$ is the valve opening degree (between 0%–100%) and A_i is the valve constant, which values are specified in Table 1. In Fig. 5 the nightly averages of the mass flow entering each evaporator are shown for the full 2.5 years period. It can be see that there is a a relative large variation in the flows for all the MT cabinets except MT_6. Noticeably, it is seen that the refrigerant flow variation in MT_6 is very small compared to any other cabinet — this is the only cabinet using modulating control rather than hysteresis control used in the other cabinets. Furthermore, the LT cabinets are seen to generally have less variation than the MT cabinets.

A plot of the one-minute values during a single night of mass flow entering the hysteresis controlled evaporator of MT_2 is shown in Fig. 6. It can be seen how the valve opens fully, which occurs when the upper cabinet temperature bound is reached, and closes again, which occurs when the lower bound is reached. In Fig. 7 the mass flow for the modulating controlled MT_6 is shown. It is seen that the flow is continuous, however around 00:30 the valve is fully opened and afterwards closed — the reason for this event is not known. To avoid disturbances e.g. customer interference, the model is fitted for all evaporators during closing hours every night from 12AM to 5AM – i.e. five hours with 300 observations as shown in the two figures.

3. Methodology

In this section grey-box model and estimation method are presented.

3.1. Modeling

The model is a state space model, derived from thermodynamic state equations describing the heat and mass dynamics of the cabinet and in the evaporator as a lumped dynamic process model [25]. As noted before, models applied in previous literature [3,22,26] were three-state models with the states: cabinet air temperature, temperature of the goods and refrigerant mass in the evaporator. In most cases this leads to parameter estimates, which are not realistic according to physics – e.g. as described in [3] the heat transfer coefficient through the walls and doors can end up very close to zero, because the goods can act as an infinite heat reservoir. Therefore, in the present study we have simplified the model by removing the state of the goods thus lumping together the cabinet air and the goods parts into a single part. The model for a single cabinet (note, that the i subscript on the variables is omitted for clarity) consists of the system equations

$$\mathrm{d}T_t^{\mathrm{c}} = \frac{1}{C_{\mathrm{c}}}\left(\frac{T_t^{\mathrm{a}} - T_t^{\mathrm{c}}}{R_{\mathrm{load}}} + M_t^{\mathrm{r}}\frac{T_t^{\mathrm{e}} - T_t^{\mathrm{c}}}{R_{\mathrm{m}}}\right)\mathrm{d}t + \sigma_{\mathrm{c}}\mathrm{d}\omega_{\mathrm{c},t} \tag{2}$$

$$\mathrm{d}M_t^{\mathrm{r}} = \left(\dot{m}_{\mathrm{in},t} - \dot{m}_{\mathrm{out},t}\right)\mathrm{d}t + \sigma_{\mathrm{r}}\mathrm{d}\omega_{\mathrm{r},t} \tag{3}$$

where $\dot{m}_{\mathrm{out},t} = \frac{M_t^{\mathrm{r}}}{R_{\mathrm{m}}\Delta h_{\mathrm{e}}}$. The latter term in each equation is the diffusion term, they are formed by the standard Wiener processes $\{\omega_{\mathrm{c},t}\}$ and $\{\omega_{\mathrm{r},t}\}$, where σ_{c} and σ_{r} become the incremental standard deviations of the processes. The ambient temperature, T_t^{a}, is an input variable , which was set constant $T_t^{\mathrm{a}} = 20°\mathrm{C}$, since measurements of the air temperature in the store were not available. The measurement equation is

$$Y_k = T_{t_k}^{\mathrm{c}} + e_k \tag{4}$$

where $e_k \sim N(0, \sigma_{\mathrm{obs}})$ and i.i.d., hence the model output is the cabinet temperature. The enthalpy difference over the evaporator, Δh_{e}, is calculated using CoolProp [27]. The deterministic part of the system equations can be illustrated by an RC-diagram [28]. A diagram for the applied model is shown in Fig. 8.

In the following presentation of the results UA-values rather than thermal resistances R are used, because they provide a more intuitive understanding ($UA = \frac{1}{R}$).

3.2. Parameter estimation

The R package, CTSM-R, is used for maximum likelihood estimation of the parameters. For all details on how the Kalman filter is used for

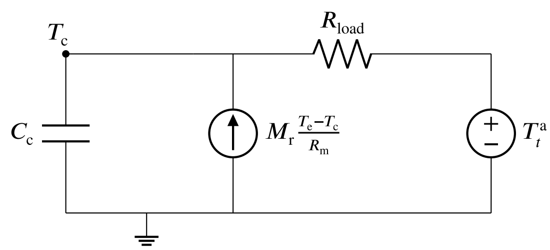

Fig. 8. RC-diagram diagram of the model. The refrigerant mass state, M_r, is included in the heat source illustrating the heat transfer to the cabinet.

state estimation and calculation of the likelihood function, and how it is maximized for the parameter estimation, see [29,30].

4. Results

In this section the obtained parameter estimates are discussed and the model is validated using an example from the fresh food refrigeration room (MT_2). The validation is carried out for the night the 9'th of July 2012, which was selected as a representative night of regular operation. The estimated parameters for the night are listed in Table 2.

It is found that the UA_{load} estimate is fairly low because it is the well insulated refrigeration room. Assuming a simple physical model of the room the UA value have been calculated based on the room specifications and physical material properties, as explained in Appendix. The calculated UA value is $31.34 \frac{W}{K}$, which is within a fair range from the estimated value $37.5 \frac{W}{K}$.

The specific heat transfer coefficient over the evaporator, UA_m, describes the rate at which the evaporator transfers heat to the cabinet — hence, it can be affected by both conditions inside the evaporator as well as on the outside e.g. obstacles such as fouling and icing.

The heat capacity of the cabinet, C_c, reflects to some extend the level of goods stored — it represents the combination of the heat capacity of the air, cabinet parts and outer layer of the goods, which responds to the temperature dynamics. The center temperature of the goods is more or less stationary. The estimated heat capacity should therefore be interpreted as the effective heat capacity, hence the heat capacity which was activated during the particular operation during the observed period.

The estimates of the diffusion terms standard deviations, σ_c and σ_r, and the measurement standard deviation, σ_{obs}, indicate that the model uncertainty is absorbed in the refrigerant mass state, since its standard deviation is much higher than the other two.

The standard error estimates (in the "Std. Error" column) indicate the accuracy of the parameter estimates. A 95% confidence interval is roughly plus and minus two times the Std. Error away from the estimate. It can be seen that the parameters are reasonably accurately determined, with standard errors roughly $\pm 10\%$ relative to the estimated values and thus certainly highly significantly different from zero.

The model performance is further analyzed by five-hour multi-step predictions of the two states. In Fig. 9 the prediction of the same night on which the estimation was carried out is shown — hence an in-sample prediction. Small issues can be seen in predicting the dynamics during the off-periods when the temperature is rising. In Fig. 10 a plot of the prediction for the following night is shown — hence an out-of-sample prediction. Here, the prediction is much worse. The reason is that the dynamics of the room have changed. From having a frequency of only 11 valve openings during the five hours, it now has 14 openings. The most plausible explanation is that fewer goods are stored in the room leading to a decreased heat capacity. Thus re-estimation of the model must be done regularly to reflect the dynamics, which change depending on the loaded goods, especially if the model is to be used for temperature prediction in a controller.

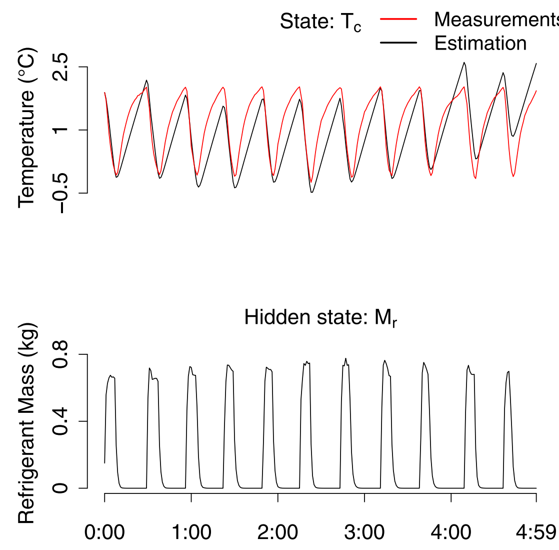

Fig. 9. Zero to five hour in-sample predictions covering the selected night (2012-06-09) for evaporator MT_2. The upper plot is of the measured cabinet temperature state and the lower is of the hidden mass state.

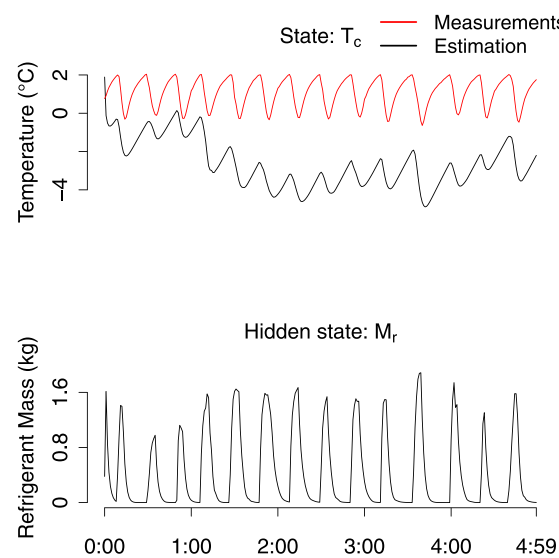

Fig. 10. Zero to five hour out-of-sample predictionscovering night following the selected night (2012-06-09) for evaporator MT_2. The upper plot is of the measured cabinet temperature state and the lower is of the hidden mass state.

Table 2
Model parameters estimated for evaporator MT_3 on the 9th of June 2012.

Parameter	Estimate	Std. Error
UA_{load} $\left[\frac{W}{K}\right]$	37.5	4.0
UA_m $\left[\frac{W}{kgK}\right]$	270.2	42.3
C_c $\left[\frac{kJ}{K}\right]$	356.5	34.6
σ_c	3.3e−12	–
σ_r	1.4	–
σ_{obs}	5.6e−11	–

4.1. Residual analysis

Diagnostic plots of the in-sample one-step prediction residuals are shown in Fig. 11. They do suggest that the model can be improved. From the two upper plots (time series and auto-correlation function (ACF)), it is seen that there is significant periodic auto-correlation in

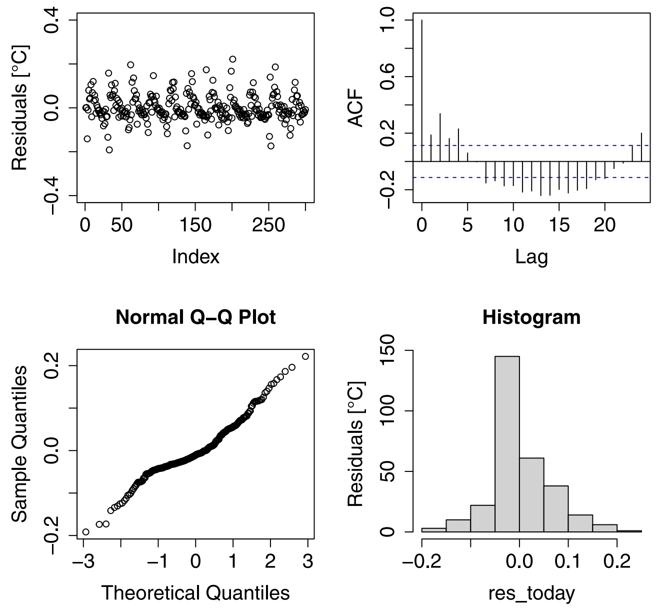

Fig. 11. Diagnostic plots of the in-sample one-step prediction residuals (2012-06-09). The upper-left plot is of the residuals, the upper-right plot is the auto-correlation function, the lower-left is the Q-Q plot and the histogram of the residuals.

the residuals, likely caused by the increasing errors during the off-period of every cycle. From the two lower plots, the QQ-plot and the histogram, it can be seen that both indicate slightly skewed residuals. For predictive applications previously presented models out-perform the current simplified model e.g. the three-state model from [3,22]. However, one issue demonstrated in [3] was the lack of robustness and more often than not the parameter estimates were not reasonable from a physical point of view, thus they could not be compared and analyzed from day to day. With the current simpler model, we were able to get consistent results and thus enabling a useful comparison of parameter estimates with some interesting potential applications – in spite of the inferior model predictions and diagnostics.

5. Parameter analysis and applications

In this section the parameter estimates for all the cabinets from the entire period, together with some suggestions of potential applications, are presented and discussed.

5.1. Cabinet classification

From the models fitted every night over the 2.5 years, a clear pattern arise in the characterization of every cabinet. In Fig. 12, the estimated heat capacities of the cabinets, C_c, are plotted versus the estimated heat transfer coefficients, UA_{load} – each dot represents the parameter estimates for a single night. It can be seen that, generally, all cabinets can be identified using these two parameters as they all clearly have distinct distributions. Furthermore, all closed cabinets are clustered with low C_c and low UA_{load}, they are the frost cabinets, LT_2, LT_3 and LT_4, along with the fresh food cabinet, MT_6. All of them are closed cabinets that are generally smaller and better insulated than open cabinets. The light blue dots represent the frost room (LT_1) – they are differentiated from the closed cabinets by having a larger heat capacity explained by its larger volume. The open cabinets and fresh storage room all have a higher variation and higher UA_{load}. Here, too, the room (red dots) has a higher heat capacity.

This analysis shows that the model and this type of data can be used to clearly differentiate between rooms, and closed and open cabinets. It

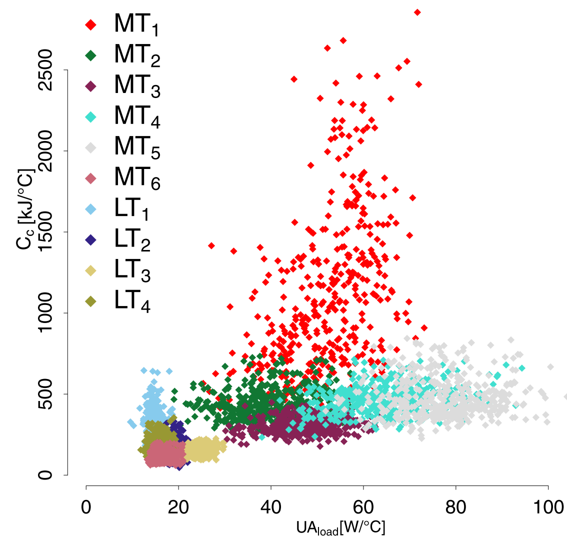

Fig. 12. Each dot represents the estimates of UA_{load} and C_c for a single cabinet during one night. It can be seen that there is a clear different pattern from the open and closed cabinets.

is useful insights into the refrigeration system that can help optimizing control settings for individual evaporators, and has potential for use in fault detection, e.g. if the parameters drift outside of their normal range. Applications which can be investigated in further research.

6. Discussion

The presented results show that useful information can be extracted from data using a rather simple grey box model. Because of its robustness and simplicity, it can be implemented as a general model on a far larger scale than previous models. The applications of the model are also different, whereas previous models primarily were derived with the objective of control, this model can be used for more informative applications, such as classification and fault detection. Without further knowledge about a supermarket refrigeration system, we can extract information about the cabinet type. Potentially, the methodology can be used to extract operational information about the systems e.g. detection of fault states (icing built-up, refrigeration leakage etc.). It is through residual analysis and tracking of the parameter estimates that cabinet outliers and faulty operation can be identified — enabling early detection of cabinets which should be repaired or replaced. Further research involving multiple supermarkets can analyze the potential for scaling up the applications. Furthermore, tracking of the heat capacity, C_c, in the storage rooms can be used to track deliveries.

These are just a few examples of the potential applications for the model, and as further research into the area drives deeper, more applications will most likely be revealed.

7. Conclusion

A grey box model describing the thermal dynamics of a supermarket refrigeration cabinet and its evaporator was presented. It was demonstrated how it, together with a maximum likelihood estimation method, can be used to extract important physical parameter estimates with data from a regular supermarket refrigeration system. The relatively simple model of the cabinet temperature was proved to be sufficient for the purpose. It was furthermore demonstrated that the parameter estimates could be used to effectively differentiate between rooms, and open and closed cabinets. This enables automatic classification of cabinets in large scale deployments. Thus further research should include data from multiple supermarkets and focus on development of classification

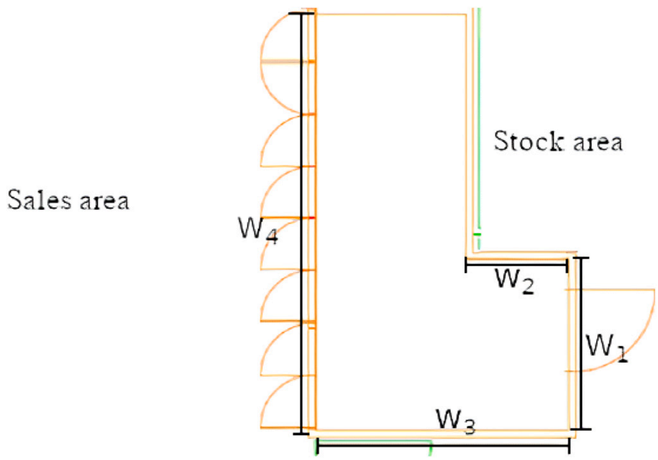

Fig. 13. Floor diagram of the refrigeration room. It has glass doors towards the sales area on the left and an insulated door to the stock area on the right. The costumers take the cold goods through the doors on the left and staff enters the room through the door on the right. Dimensions used in the calculations are marked.

models using the parameter estimates as input. Possible applications, such as tracking of abnormal cabinet operation for early fault detection, should also be investigated in follow-up studies.

CRediT authorship contribution statement

K. Leerbeck: Conceptualization, Methodology, Software, Writing. **P. Bacher:** Conceptualization, Methodology, Supervision, Writing. **C. Heerup:** Data curation, Supervision, Review.

Declaration of competing interest

One or more of the authors of this paper have disclosed potential or pertinent conflicts of interest, which may include receipt of payment, either direct or indirect, institutional support, or association with an entity in the biomedical field which may be perceived to have potential conflict of interest with this work. For full disclosure statements refer to https://doi.org/10.1016/j.egyai.2022.100211. Kenneth Leerbeck reports financial support was provided by Danish Energy Agency. Peder Bacher reports financial support was provided by Danish Energy Agency. Christian Heerup reports financial support was provided by Danish Energy Agency. Henrik Madsen reports financial support was provided by Danish Energy Agency.

Data availability

The authors do not have permission to share data.

Acknowledgment & funding

This document is the results of the research projects *Digital twins for large-scale heat pumps and refrigeration systems* (EUDP 64019-0570) and *Flexible Energy Denmark (FED)* (IFD 8090-00069B).

Appendix. UA calculation for fresh food refrigeration room.

The refrigeration room has glass towards the sales area on the left. It has a thick insulated door towards the storage area to the right. The walls and the door towards the storage room have 7 cm of insulation in the walls and the glass doors are 2 cm thick (properties used for walls: $\lambda = 0.022$ W/(mK) & $H = 2.5$ m, and for glass doors: $U = 1.1$ W/K & $H = 2$ m). Data about the room is listed in Table 3. The walls are referred to as W and use the same numbering as in Fig. 13.

Table 3
Room specifications: W is the width of the section and the area, A, is calculated from the room height, $H = 2.5$ m. The heat transfer coefficient, UA, is calculated in two parts — first, the total area of the parts with insulation (walls and roof) then the total area of the glass doors ($UA = \left(\frac{A}{\frac{L}{k}}\right)$).

Parameter	W [m]	A [m^2]	UA [W/K]
Insulated walls, door and roof			
W_1	2.8 m		
W_2	1.5 m		
W_3	3.9 m		
W_4	6.3 m		
Roof		20.37 m^2	
Total		55.62 m^2	17.48 W/K
Glass doors			
Total	3.9 m	12.6 m^2	13.86 W/K
Complete room			
Total			**31.34 W/K**

The wall widths are listed under W and the areas calculated under A. The heat transfer coefficient, UA, is calculated in two parts — first, the total area of the parts with insulation (walls and roof) then the total area of the glass doors.

References

[1] Jiang Y, Yin S, Li K, Luo H, Kaynak O. Industrial applications of digital twins. Phil Trans R Soc A 2021;379.
[2] Brok Niclas Brabrand, Munk-Nielsen Thomas, Madsen Henrik, Stentoft Peter A. Flexible control of wastewater aeration for cost-efficient, sustainable treatment. IFAC-PapersOnLine 2019;52(4):494–9, IFAC Workshop on Control of Smart Grid and Renewable Energy Systems CSGRES 2019.
[3] Leerbeck Kenneth, Bacher Peder, Heerup Christian. Grey box modelling of supermarket refrigeration room. In: Proceedings of the 2021 international conference on electrical, computer and energy technologies. European Union; 2021, 2021 International Conference on Electrical, Computer and Energy Technologies, ICECET 2021 ; Conference date: 09-12-2021 Through 10-12-2021.
[4] Glavan Miha, Gradišar Dejan, Moscariello Salvatore, Juričić Ðani, Vrančić Damir. Demand-side improvement of short-term load forecasting using a proactive load management – a supermarket use case. Energy Build 2019;186:186–94.
[5] Brok Niclas, Green Torben, Heerup Christian, Oren Shmuel S, Madsen Henrik. Optimal operation of an ice-tank for a supermarket refrigeration system. Control Eng Pract 2022;119:104973.
[6] Li Yanfei, Sun Jian, Fricke Brian, Im Piljae, Kuruganti Teja. Grey-box fault models and applications for low carbon emission CO2 refrigeration system. Int J Refrig 2022;141:76–89.
[7] Kristensen Niels Rode, Madsen Henrik, Jørgensen Sten Bay. A method for systematic improvement of stochastic grey-box models. Comput Chem Eng 2004;28(8):1431–49.
[8] Maruta Ichiro, Sugie Toshiharu. Projection-based identification algorithm for grey-box continuous-time models. Systems Control Lett 2013;62(11):1090–7.
[9] Nielsen Jan Nygaard, Madsen Henrik, Young Peter C. Parameter estimation in stochastic differential equations: An overview. Annu Rev Control 2000;24:83–94.
[10] Bacher Peder, Madsen Henrik. Identifying suitable models for the heat dynamics of buildings. Energy Build 2011;43(7):1511–22.
[11] Kim Donghun, Cai Jie, Braun James E, Ariyur Kartik B. System identification for building thermal systems under the presence of unmeasured disturbances in closed loop operation: Theoretical analysis and application. Energy Build 2018;167:359–69.
[12] Kizilkan Önder. Thermodynamic analysis of variable speed refrigeration system using artificial neural networks. Expert Syst Appl 2011;38(9):11686–92.
[13] Cirera Josep, Carino Jesus A, Zurita Daniel, Ortega Juan A. Improving the energy efficiency of industrial refrigeration systems by means of data-driven load management. Processes 2020;8(9).
[14] Pérez-Segarra CD, Rigola J, Sòria M, Oliva A. Detailed thermodynamic characterization of hermetic reciprocating compressors. Int J Refrig 2005;28:579–93.
[15] Willatzen M, Pettit NBOL, Ploug-Sørensen L. A general dynamic simulation model for evaporators and condensers in refrigeration. Part I: moving-boundary formulation of two-phase flows with heat exchange. Int J Refrig 1998;21:398–403.
[16] Corradi M, Cecchinato L, Schiochet G, Zilio C. Modelling fin-and-tube gas-cooler for transcritical carbon dioxide cycles. In: International refrigeration and air conditioning. 2006.

[17] Aprea C, Renno C. An experimental analysis of a thermodynamic model of a vapor compression refrigeration plant on varying the compressor speed. Int J Energy Res 2004;28:537–49.

[18] Wang F, Maidment G, Missenden J, Tozer R. The novel use of phase change materials in refrigeration plant. Part 2: Dynamic simulation model for the combined system. Appl Therm Eng 2007;27:2902–10.

[19] Zhou R, Zhang T, Catano J, Wen JT, Michna G J, Peles Y, et al. The steady-state modeling and optimization of a refrigeration system for high heat flux removal. Appl Therm Eng 2010;30:2347–56.

[20] Andreasen G, Stoustrup J, Izadi-Zamanabadi R, Pardiñas Á, Hafner A. Data-driven modeling of a CO2 refrigeration system. In: American control conference. 2019.

[21] Katayama T. Subspace methods for system identification. Springer; 2005.

[22] Shafiei E, Rasmussen H, Skoustrup J. Modeling supermarket refrigeration systems for demand-side management. Energies 2013;6:900–20.

[23] Fredslund K. Load profiles for supermarket refrigeration. Technical Report, IPU; 2013, p. 75.

[24] Leerbeck Kenneth, Bacher Peder, Heerup Christian, Madsen Henrik. Estimation of evaporator valve sizes in supermarket refrigeration cabinets. 2022.

[25] Madsen Henrik. Time series analysis. Chapman & Hall/CRC - Taylor & Francis Group; 2007.

[26] Sarabia D, Capraro F, Larsen LFS, de Prada C. Hybrid NMPC of supermarket display cases. Control Eng Pract 2009;17:428–41.

[27] Bell Ian H, Wronski Jorrit, Quoilin Sylvain, Lemort Vincent. Pure and pseudo-pure fluid thermophysical property evaluation and the open-source thermophysical property library CoolProp. Ind Eng Chem Res 2014;53(6):2498–508.

[28] Madsen H, Holst J. Estimation of continuous-time models for the heat dynamics of a building. Energy Build 1995;22(1):67–79.

[29] Madsen Henrik. Continuous time stochastic modeling in R - user's guide and reference manual. CTSM-R Development Team; 2003.

[30] Kristensen Niels Rode, Madsen Henrik, Jørgensen Sten Bay. Parameter estimation in stochastic grey-box models. Automatica 2004;40(2):225–37.